Inorganic Chemistry
Article

Inorg. Chem. **2010**, *49*, 6509–6517 **6509**
DOI: 10.1021/ic100245a

Binuclear Hexa- and Pentavalent Uranium Complexes with a Polypyrrolic Ligand: A Density Functional Study of Water- and Hydronium-Induced Reactions

Qing-Jiang Pan[†,‡] and Georg Schreckenbach*[,†]

[†]*Department of Chemistry, University of Manitoba, Winnipeg, MB, Canada R3T 2N2, and* [‡]*Key Laboratory of Functional Inorganic Material Chemistry of Education Ministry and Laboratory of Physical Chemistry, School of Chemistry and Materials Science, Heilongjiang University, Harbin, China 150080*

Received February 5, 2010

Binuclear uranyl (VI) and (V) complexes of a Pacman-like polypyrrolic macrocycle (H_4L) were investigated using relativistic density functional theory. The reactivity of the bis-uranyl(VI) complex $(UO_2)_2(L)$ (**2a**) was explored computationally. Although **2a** has not been obtained experimentally, its structural analogue $[(UO_2)(OH)K(THF)_2(H_2L^{Me})]$ has been synthesized recently. The high reactive activity of **2a** originates from its unique butterfly like cation−cation structure, containing an active O center with easily broken U−O bonding and having unsaturated coordination sites of uranium(VI) along the equatorial plane. The present study indicates that **2a** can react with water (Path 3) and hydronium (Path 4), which lead to the formation of a series of complexes with a triangle-like O═U═O═U═O skeleton. Path 3 results in an unusual complex containing a combined *cis*-uranyl/*trans*-uranyl cation−cation structure, (*cis*-UO_2)(*trans*-UO_2)(H_2O)(L) (**4b**), where the oxo atom of the *trans*-uranyl coordinates the uranium center of the *cis*-uranyl and the water bonds to the uranium of *trans*-uranyl in the equatorial plane. After a process of hydrogen transfer with an extremely low energy barrier (<1.5 kcal/mol), **4b** is converted into a slightly more stable isomer $(U_2O_3)(OH)_2(L)$ (**4a**), where two hydroxyl groups link to two uranium atoms, respectively. In conjunction with previous studies, the free energies of reactions of **2a** induced by isomerization (Path 1), proton (Path 2), water (Path 3), and hydronium (Path 4) were calculated in the gas phase and aqueous solution. Solvation stabilizes the free energy of the formation reactions of the neutral complexes but destabilizes that of the charged complexes. In these reactions, three pairs of isomers were obtained for binuclear uranium(VI) complexes, but only the most stable in each pair exists for the binuclear uranium(V) analogues.

1. Introduction

The early 5f-elements such as uranium, neptunium, and plutonium have interesting electronic and structural properties that arise from the accessibility of the s, p, d, and f orbitals to chemical bonding, thus allowing for exciting coordination chemistry.[1,2] By far the most stable form of uranium in most processing and environmental conditions is the uranyl ion, UO_2^{2+}, which exists as a linear dication with 4 to 6 ligands in the equatorial plane.[3−10] The linear *trans*-uranyl structure is predominant in all the reported uranyl crystalline complexes,[3−9] whereas *cis*-uranyl complexes were predicted only by theory[11] except for a controversial report on a *cis*-uranyl polymer, $[UO_2(Fcdc)(THF)(Fc)]$ (Fcdc = 1,2-ferrocenedicarboxylate, Fc = ferrocene).[12,13] Apart from its fundamental interest, the uranyl ion UO_2^{2+} has important environmental implications.[14] The highly soluble and mobile UO_2^{2+} species are key players in the long term

*To whom correspondence should be addressed. E-mail: schrecke@cc.umanitoba.ca.

(1) Kaltsoyannis, N.; Scott, P. *The f elements*; Oxford Science Publications; Oxford University Press: New York, 1999.
(2) Bart, S. C.; Meyer, K. Highlights in uranium coordination chemistry. In *Organometallic and Coordination Chemistry of the Actinides*; Springer-Verlag Berlin: Berlin, 2008; Vol. *127*, pp 119−176.
(3) Berthet, J. C.; Lance, M.; Nierlich, M.; Ephritikhine, M. *Eur. J. Inorg. Chem.* **2000**, 1969–1973.
(4) Berthet, J. C.; Nierlich, M.; Ephritikhine, M. *Chem. Commun.* **2003**, 1660–1661.
(5) Berthet, J. C.; Nierlich, M.; Ephritikhine, M. *Chem. Commun.* **2004**, 870–871.
(6) Berthet, J. C.; Nierlich, M.; Ephritikhine, M. *Angew. Chem., Int. Ed.* **2003**, *42*, 1952–1954.
(7) Oldham, W. J.; Oldham, S. M.; Scott, B. L.; Abney, K. D.; Smith, W. H.; Costa, D. A. *Chem. Commun.* **2001**, 1348–1349.
(8) Vaughn, A. E.; Barnes, C. L.; Duval, P. B. *J. Chem. Crystallogr.* **2007**, *37*, 779–782.
(9) Alcock, N. W.; Flanders, D. J.; Brown, D. *J. Chem. Soc., Dalton Trans.* **1985**, 1001–1007.
(10) Wilkerson, M. P.; Burns, C. J.; Paine, R. T.; Scott, B. L. *Inorg. Chem.* **1999**, *38*, 4156–4158.
(11) Schreckenbach, G.; Hay, P. J.; Martin, R. L. *Inorg. Chem.* **1998**, *37*, 4442–4451.
(12) Vaughn, A. E.; Barnes, C. L.; Duval, P. B. *Angew. Chem., Int. Ed.* **2007**, *46*, 6622–6625.
(13) Villiers, C.; Thuery, P.; Ephritikhine, M. *Angew. Chem., Int. Ed.* **2008**, *47*, 5892–5893.
(14) Hashke, J. M.; Stakebake, J. L. Handling, storage, and disposition of plutonium and uranium. In *The chemistry of the actinide and transactinide elements*; Morss, L. R., Edelstein, N. M., Fuger, J., Eds.; Springer: New York, 2006; pp 3199−3272.

Published on Web 06/17/2010

environmental risks associated with the disposal of radioactive waste. Therefore, a greater understanding of uranyl coordination chemistry is essential, technologically, for the safe processing and long-term immobilization of irradiated radionuclides.

In contrast to the coordination chemistry of actinyl(VI) cations, actinyl(V) cations are well-known to participate in cation−cation interactions (CCI) where the oxo atom of one actinyl unit coordinates the actinyl metal center of another.[15−25] Recently, CCI has been recognized in U(VI) chemistry also.[26−31] These interactions play a significant role in the fields of solution and solid-state chemistry of AnO_2^{n+},[26−36] where they can lead to the formation of dimers,[15−20] oligomers,[24−26] one-dimensional and multidimensional networks[27−36] that do not necessarily require the support of ancillary ligands. The synthesis and characterization of a number of complexes with an $AnO_2^{n+}\cdots M^{m+}$ (where M is an alkali metal[37,38] or transition metal[39−42]) structure can be viewed as an extension of this kind of interaction.

Pentavalent UO_2^+ is known to readily disproportionate in water to form U(IV) and UO_2^{2+}, whereas other actinides (Np, Pu, Am) form stable AnO_2^+ species that can easily be isolated in crystalline complexes.[20,21,43] Careful choice of equatorial coordination ligands can lead to the formation of pentavalent uranyl complexes such as $\{[UO_2Py_5][KI_2Py_2]\}_n$[37] or $\{[U^VO_2(dbm)_2]_4[K_6Py_{10}]\}\cdot I_2\cdot Py_2$ (dbm = dibenzoylmethanate)[24] and its derivatives.[25]

Besides the use of multiple ligands,[3−10] expanded porphyrins and related macrocycles[44−49] are prospective ligands for actinyl complexation. The Love[49−55] and Sessler[56,57] groups have synthesized a flexible macrocylic ligand

Scheme 1. Theoretically Predicted Formation Path of $(UO_2)(H_2L)(THF)$ (**1**) and $(UO_2)_2(L)$ (Butterfly-Like **2a** and T-Shaped **2b**) from ref 64[a]

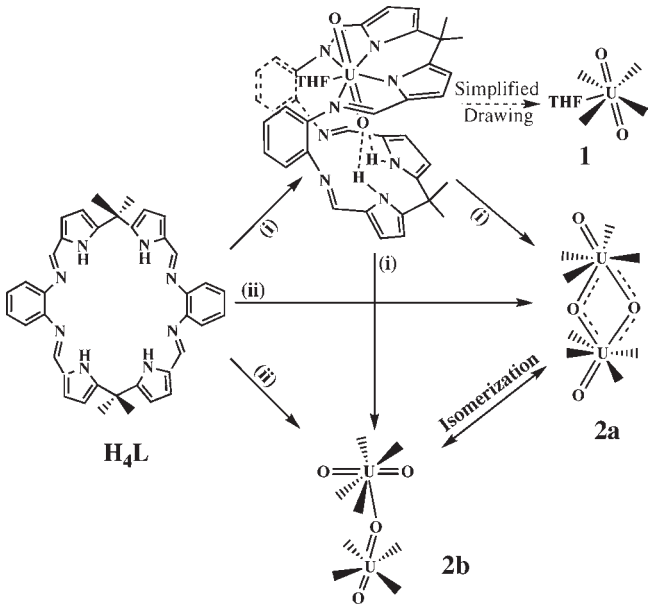

[a] The uranyl reagent, (i) $[UO_2(H_2O)_5]^{2+}$ and (ii) $2\cdot[UO_2(H_2O)_5]^{2+}$, was used in the calculations.

(15) Sullivan, J. C.; Zielen, A. J.; Hindman, J. C. *J. Am. Chem. Soc.* **1961**, *83*, 3373–3378.
(16) Guillaume, B.; Begun, G. M.; Hahn, R. L. *Inorg. Chem.* **1982**, *21*, 1159–1166.
(17) Guillaume, B.; Hahn, R. L.; Narten, A. H. *Inorg. Chem.* **1983**, *22*, 109–111.
(18) Nagasaki, S.; Kinoshita, K.; Enokida, Y.; Suzuki, A. *J. Nucl. Sci. Technol.* **1992**, *29*, 1100–1107.
(19) Den Auwer, C.; Gregoire-Kappenstein, A. C.; Moisy, P. *Radiochim. Acta* **2003**, *91*, 773–776.
(20) Grigoriev, M. S.; Krot, N. N.; Bessonov, A. A.; Suponitsky, K. Y. *Acta Crystallogr., Sect. E.: Struct. Rep. Online* **2007**, *63*, M561–M562.
(21) Charushnikova, I. A.; Krot, N. N.; Polyakova, I. N. *Crystallogr. Rep.* **2006**, *51*, 201–204.
(22) Reilly, S. D.; Neu, M. P. *Inorg. Chem.* **2006**, *45*, 1839–1846.
(23) Gorden, A. E. V.; Xu, J. D.; Raymond, K. N.; Durbin, P. *Chem. Rev.* **2003**, *103*, 4207–4282.
(24) Burdet, F.; Pecaut, J.; Mazzanti, M. *J. Am. Chem. Soc.* **2006**, *128*, 16512–16513.
(25) Nocton, G.; Horeglad, P.; Pecaut, J.; Mazzanti, M. *J. Am. Chem. Soc.* **2008**, *130*, 16633–16645.
(26) Wilkerson, M. P.; Burns, C. J.; Dewey, H. J.; Martin, J. M.; Morris, D. E.; Paine, R. T.; Scott, B. L. *Inorg. Chem.* **2000**, *39*, 5277–5285.
(27) Sullens, T. A.; Jensen, R. A.; Shvareva, T. Y.; Albrecht-Schmitt, T. E. *J. Am. Chem. Soc.* **2004**, *126*, 2676–2677.
(28) Alekseev, E. V.; Krivovichev, S. V.; Depmeier, W.; Siidra, O. I.; Knorr, K.; Suleimanov, E. V.; Chuprunov, E. V. *Angew. Chem., Int. Ed.* **2006**, *45*, 7233–7235.
(29) Alekseev, E. V.; Krivovichev, S. V.; Malcherek, T.; Depmeier, W. *Inorg. Chem.* **2007**, *46*, 8442–8444.
(30) Alekseev, E. V.; Krivovichev, S. V.; Depmeier, W.; Armbruster, T.; Katzke, H.; Suleimanov, E. V.; Chuprunov, E. V. *J. Solid State Chem.* **2006**, *179*, 2977–2987.
(31) Kubatko, K. A.; Burns, P. C. *Inorg. Chem.* **2006**, *45*, 10277–10281.
(32) Forbes, T. Z.; Burns, P. C.; Soderholm, L.; Skanthakumar, S. *Chem. Mater.* **2006**, *18*, 1643–1649.
(33) Almond, P. M.; Skanthakumar, S.; Soderholm, L.; Burns, P. C. *Chem. Mater.* **2007**, *19*, 280–285.
(34) Forbes, T. Z.; Burns, P. C. *J. Solid State Chem.* **2007**, *180*, 106–112.
(35) Forbes, T. Z.; Burns, P. C. *J. Solid State Chem.* **2009**, *182*, 43–48.
(36) Albrecht-Schmitt, T. E.; Almond, P. M.; Sykora, R. E. *Inorg. Chem.* **2003**, *42*, 3788–3795.
(37) Natrajan, L.; Burdet, F.; Pecaut, J.; Mazzanti, M. *J. Am. Chem. Soc.* **2006**, *128*, 7152–7153.
(38) Burns, C. J.; Clark, D. L.; Donohoe, R. J.; Duval, P. B.; Scott, B. L.; Tait, C. D. *Inorg. Chem.* **2000**, *39*, 5464–5468.
(39) Thuery, P. *Inorg. Chem. Commun.* **2009**, *12*, 800–803.
(40) Ekstrom, A.; Farrar, Y. *Inorg. Chem.* **1972**, *11*, 2610–2615.
(41) Sullivan, J. C. *J. Am. Chem. Soc.* **1962**, *84*, 4256–4259.
(42) Newton, T. W.; Burkhart, M. J. *Inorg. Chem.* **1971**, *10*, 2323–2326.
(43) Katz, J. J.; Morss, L. R.; Seaborg, G. T. In *The Chemistry of the Actinide Elements*; Chapman and Hall: London, 1986.
(44) Sessler, J. L.; Hemmi, G.; Mody, T. D.; Murai, T.; Burrell, A.; Young, S. W. *Acc. Chem. Res.* **1994**, *27*, 43–50.
(45) Sessler, J. L.; Vivian, A. E.; Seidel, D.; Burrell, A. K.; Hoehner, M.; Mody, T. D.; Gebauer, A.; Weghorn, S. J.; Lynch, V. *Coord. Chem. Rev.* **2001**, *216*, 411–434.
(46) Sessler, J. L.; Melfi, P. J.; Pantos, G. D. *Coord. Chem. Rev.* **2006**, *250*, 816–843.
(47) Chang, C. J.; Baker, E. A.; Pistorio, B. J.; Deng, Y. Q.; Loh, Z. H.; Miller, S. E.; Carpenter, S. D.; Nocera, D. G. *Inorg. Chem.* **2002**, *41*, 3102–3109.
(48) Pistorio, B. J.; Chang, C. J.; Nocera, D. G. *J. Am. Chem. Soc.* **2002**, *124*, 7884–7885.
(49) Love, J. B. *Chem. Commun.* **2009**, 3154–3165.
(50) Givaja, G.; Volpe, M.; Edwards, M. A.; Blake, A. J.; Wilson, C.; Schroder, M.; Love, J. B. *Angew. Chem., Int. Ed.* **2007**, *46*, 584–586.
(51) Givaja, G.; Volpe, M.; Leeland, J. W.; Edwards, M. A.; Young, T. K.; Darby, S. B.; Reid, S. D.; Blake, A. J.; Wilson, C.; Wolowska, J.; McInnes, E. J. L.; Schroder, M.; Love, J. B. *Chem.—Eur. J.* **2007**, *13*, 3707–3723.
(52) Givaja, G.; Blake, A. J.; Wilson, C.; Schroder, M.; Love, J. B. *Chem. Commun.* **2005**, 4423–4425.
(53) Givaja, G.; Blake, A. J.; Wilson, C.; Schroder, M.; Love, J. B. *Chem. Commun.* **2003**, 2508–2509.
(54) Volpe, M.; Hartnett, H.; Leeland, J. W.; Wills, K.; Ogunshun, M.; Duncombe, B. J.; Wilson, C.; Blake, A. J.; McMaster, J.; Love, J. B. *Inorg. Chem.* **2009**, *48*, 5195–5207.
(55) Volpe, M.; Reid, S. D.; Blake, A. J.; Wilson, C.; Love, J. B. *Inorg. Chim. Acta* **2007**, *360*, 273–280.
(56) Veauthier, J. M.; Tomat, E.; Lynch, V. M.; Sessler, J. L.; Mirsaidov, U.; Markert, J. T. *Inorg. Chem.* **2005**, *44*, 6736–6743.
(57) Veauthier, J. M.; Cho, W. S.; Lynch, V. M.; Sessler, J. L. *Inorg. Chem.* **2004**, *43*, 1220–1228.

Scheme 2. Theoretically Predicted Reaction Paths of Binuclear U(VI) Complexes[a]

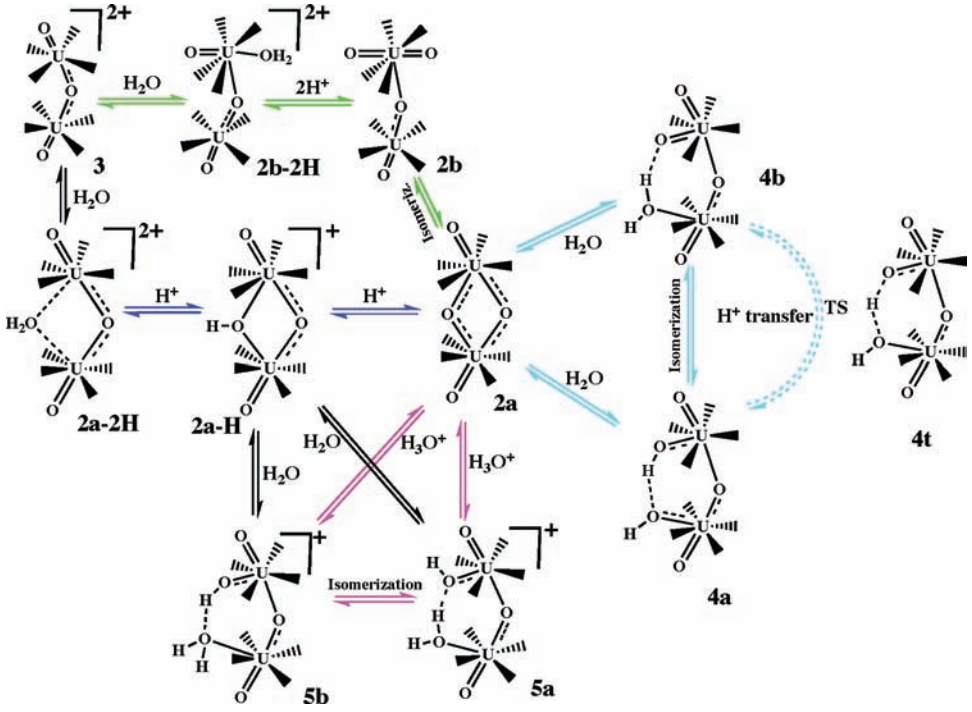

[a] Path 1: **2a**↔**2b**↔**2b-2H**↔**3** (green color); Path 2: **2a**↔**2a-H**↔**2a-2H** (blue); Path 3: **2a**↔**4a**↔**4t**↔**4b** (cyan); and Path 4: **2a**↔**5a**↔**5b** (magenta); the overall charges were added except for the neutral complexes.

H_4L (Scheme 1), in which the cavity is large enough to coordinate two transition metals. The aryl groups in the macrocycle function as hinges that result in a rigid molecular cleft structure, often called a "Pacman" structure.[47,48,58] The studies of Arnold and Love have shown that the reaction of H_4L with uranyl silylamides yields mononuclear complexes $(UO_2)(THF)(H_2L)$ (**1**),[59] heterobinuclear complexes $[(THF)UO_2\cdots M(THF)](L)$ (M = Mn, Fe and Co),[60] and their one-electron reduced uranium(V) products.[61−63] Our recent theoretical investigation[64] showed that the unique Pacman-like ligand is in principle able to accommodate two uranyl ions to form two possible bis-uranyl isomeric complexes $(UO_2)_2(L)$, with butterfly like (**2a**) and T-shaped (**2b**) structures. Although these structures have not yet been obtained experimentally, the complex $[(UO_2)(OH)K(THF)_2(H_2L^{Me})]$,[65] structurally resembling **2a**, has been synthesized recently.

In the current paper, we have designed additional reactions induced by water and hydronium to provide insight into the reactivity of such binuclear complexes. These reactions result in the formation of a series of complexes with a triangle-like O=U=O=U=O skeleton. The explicit and implicit solvent effects were taken into account in the present calculations, and thus, the free energy of formation reaction for each binuclear uranium(VI) complex was estimated. In addition, binuclear uranium(V) analogues corresponding to their binuclear uranium(VI) complexes were obtained successfully, which provides computational evidence that the polypyrrolic ligand can stabilize U(V) species.

2. Scope and Computational Details

Scope of the Current Study. As shown in Scheme 1,[64] mononuclear **1** and binuclear **2a** and **2b** can be formed by reactions of uranyl species with the polypyrrolic ligand. The protonation reactions of binuclear complexes (Path 1 and Path 2 in Scheme 2) were previously studied theoretically in the gas phase.[64] Herein, two more reaction pathways induced by water (Path 3) and hydronium (Path 4) have been investigated, starting from complex **2a**. In contrast to the previous gas-phase calculations, explicit and implicit solvent effects have also been considered. Therefore, the free energy of formation reaction for each binuclear uranium(VI) complex in Paths 1 to 4 was estimated and compared in the gas phase and in solution. In these reactions, we obtained a series of possible products, $[(U_2O_4H)(L)]^+$ (**2a-H**), $[(U_2O_3)(H_2O)(L)]^{2+}$ (**2a-2H** and **2b-2H**), $[(U_2O_3)(L)]^{2+}$ (**3**), $(U_2O_3)(OH)_2(L)$ (**4a**), (*cis*-UO_2)(*trans*-UO_2)$(H_2O)(L)$ (**4b**), $(UO_2)_2(O)(H)(OH)(L)$ (**4t**), $[(U_2O_3)(HO)(HOH)(L)]^+$ (**5a**), and $[(U_2O_3)(OH)(OH_2)(L)]^+$ (**5b**). The structures of the newly optimized **4a**, **4b**, **4t**, **5a**, and **5b** will be discussed in detail. In addition, the study of binuclear uranium(V) complexes, $[(UO_2)_2(L)]^{2-}$ (**6**), $[(U_2O_3)(OH)_2(L)]^{2-}$ (**7**), and $[(U_2O_3)(HO)(HOH)(L)]^-$ (**8**) showed that the Pacman-like ligand is able to stabilize the UO_2^+ ion, in agreement with the experimentally reported uranyl(V) polypyrrolic complex.[61]

(58) Collman, J. P.; Wagenknecht, P. S.; Hutchison, J. E. *Angew. Chem., Int. Ed.* **1994**, *33*, 1537–1554.
(59) Arnold, P. L.; Blake, A. J.; Wilson, C.; Love, J. B. *Inorg. Chem.* **2004**, *43*, 8206–8208.
(60) Arnold, P. L.; Patel, D.; Blake, A. J.; Wilson, C.; Love, J. B. *J. Am. Chem. Soc.* **2006**, *128*, 9610–9611.
(61) Arnold, P. L.; Patel, D.; Wilson, C.; Love, J. B. *Nature* **2008**, *451*, 315–318.
(62) Arnold, P. L.; Love, J. B.; Patel, D. *Coord. Chem. Rev.* **2009**, *253*, 1973–1978.
(63) Yahia, A.; Arnold, P. L.; Love, J. B.; Maron, L. *Chem. Commun.* **2009**, 2402–2404.
(64) Pan, Q. J.; Shamov, G. A.; Schreckenbach, G. *Chem.—Eur. J.* **2010**, *16*, 2282–2290.
(65) Arnold, P. L.; Patel, D.; Pecharman, A. F.; Wilson, C.; Love, J. B. *Dalton Trans.* **2010**, *39*, 3501–3508.

Computational Details. Unless otherwise noted, all the calculations were accomplished by the Priroda code (Version 6).[66−70] Relativistic effects were implemented using a scalar relativistic four-component all-electron approach,[71] which is based on the full Dirac equation but with spin−orbit projected out[72] and neglected. Because the oxidation state of uranium(VI) is kept constant in these reactions, this approximation is valid.[73] All-electron Gaussian correlation-consistent basis sets of triple-ζ polarized quality (TZP) for the large component, the corresponding kinetically balanced basis sets for the small component, and corresponding Coulomb/exchange optimized fitting basis sets were used.[68,69]

We performed the calculations using approximate density functional theory (DFT) in the form of the PBE exchange-correlation functional,[74] that is, a generalized gradient approximation (GGA) version of DFT. All structures were optimized in the gas phase without any symmetry constraints. Subsequent analytical frequency calculations were used to confirm the nature of the stationary points on the potential energy surface and also to obtain thermodynamic data. Population-based (Mayer) bond orders[75] and atomic charges as developed by Hirshfeld[76] were calculated based on these PBE calculations. Because of the use of the resolution-of-identity (RI) approximation,[67] the Priroda code has been successfully applied to calculate large molecular systems at the DFT level, and is thus particularly advantageous for calculations on actinide complexes.[73,77−83] Careful comparisons with other relativistic methods as implemented in codes such as Gaussian 03 and ADF confirmed that Priroda is entirely reliable for actinide complexes.[73,79−81] Recent investigations of binuclear $UO_2^{2+}\cdots M^{2+}$ (An = U, Np and Pu; M = Mn, Fe, Co and Zn) complexes of the same macrocycle have given reasonable agreement with experimental results.[82]

To obtain the free energies of solvation, the ADF 2008.01 code[84−86] was used in the calculations. An integration parameter of 6.0 was applied. The solvent effects of water were taken into account by the COSMO model as implemented in ADF.[87] Klamt radii were used for the main group atoms (H = 1.30 Å, C = 2.00 Å, N = 1.83 Å, and O = 1.72 Å)[88] and for the actinide atom (U = 1.70 Å). The scalar relativistic ZORA method[89−91] was applied in the ADF calculations. ZORA-TZP basis sets, similar in quality to those applied in the Priroda calculations, and the same PBE XC functional were used.

Structures **1** and **2a** were taken as examples to be reoptimized using the ADF code in the gas phase and solution, to assess the performance of the Priroda-optimized (gas-phase) geometries. The optimized results of Priroda in the gas phase (labeled as Pri-gas), ADF in the gas phase (ADF-gas), and ADF in solution (ADF-sol) are listed in the Supporting Information, Table S1. On the basis of the Pri-gas and ADF-gas geometries, the solvation free energies were obtained in single-point ADF-COSMO calculations. From these studies, we draw the following conclusions (Supporting Information, Table S1): (i) the difference in geometry parameters between Pri-gas and ADF-gas is negligible; for instance, the difference between the $U{=}O_{exo}$ bond lengths amounts to less than 0.001 Å; (ii) a small relaxation (e.g., ca. 0.01 Å for $U{=}O_{exo}$) is seen in going from ADF-gas to ADF-sol optimization; (iii) the difference in solvation free energies (ΔG(sol)) is less than 0.4 kcal/mol between the Pri-gas and ADF-gas optimized geometries, and about 1.5 kcal/mol stabilization of ΔG(sol) is achieved from ADF-gas to ADF-sol. Because all reagents and products become slightly stabilized due to the ADF solution optimization, error cancelation ensures that such stabilization does not change the free energies of the whole reaction. Therefore, in the remainder of this work, we report single-point ADF-COSMO calculations on Priroda-optimized (gas-phase) geometries to obtain solvation free energies, without reoptimization using ADF.

3. Results and Discussion

3.1. Geometrical Structures and Bond Orders of Binuclear Uranium(VI) Complexes. As seen in Scheme 1, the reaction of the polypyrrolic ligand with uranyl species results in the experimentally known mononuclear **1**.[59] When we put two uranyl ions into the cavity of the ligand, full optimization indicates that binuclear isomers (butterfly like **2a** and T-shaped **2b**) are theoretically stable.[64] **2a** and **2b** can also be obtained from mononuclear **1** upon further reaction with uranyl species.

Four paths were designed to explore reactivity under different conditions (Scheme 2). The more stable isomer **2a** is potentially reactive because it has a special butterfly like cation−cation structure, where the $O{=}U\text{-}(O)_2\text{-}U{=}O$ part contributes an active and exposed O center with easily broken U−O bonding. Moreover, it contains

(66) Laikov, D. N. *J. Comput. Chem.* **2007**, *28*, 698–702.
(67) Laikov, D. N.; Ustynyuk, Y. A. *Russ. Chem. Bull.* **2005**, *54*, 820–826.
(68) Laikov, D. N. *Chem. Phys. Lett.* **2005**, *416*, 116–120.
(69) Laikov, D. N., Ph.D. Thesis, Moscow State University, Moscow, 2000.
(70) Laikov, D. N. *Chem. Phys. Lett.* **1997**, *281*, 151–156.
(71) Laikov, D. N. *An Implementation of the Scalar Relativistic Density Functional Theory for Molecular Calculations with Gaussian Basis Sets*; DFT2000 Conference: Menton, France, 2000.
(72) Dyall, K. G. *J. Chem. Phys.* **1994**, *100*, 2118–2127.
(73) Shamov, G. A.; Schreckenbach, G. *J. Am. Chem. Soc.* **2008**, *130*, 13735–13744.
(74) Perdew, J. P.; Burke, K.; Ernzerhof, M. *Phys. Rev. Lett.* **1996**, *77*, 3865–3868.
(75) Mayer, I. *Simple theorems, proof and derivations in quantum chemistry*; Kluwer Academic/Plenum Publishers: New York, 2003.
(76) Hirshfeld, F. L. *Theor. Chim. Acta* **1977**, *44*, 129–138.
(77) Shamov, G. A.; Schreckenbach, G.; Martin, R. L.; Hay, P. J. *Inorg. Chem.* **2008**, *47*, 1465–1475.
(78) Shamov, G. A.; Schreckenbach, G. *Inorg. Chem.* **2008**, *47*, 805–811.
(79) Shamov, G. A.; Schreckenbach, G.; Vo, T. N. *Chem.—Eur. J.* **2007**, *13*, 4932–4947.
(80) Shamov, G. A.; Schreckenbach, G. *J. Phys. Chem. A* **2006**, *110*, 9486–9499.
(81) Shamov, G. A.; Schreckenbach, G. *J. Phys. Chem. A* **2005**, *109*, 10961–10974. (Correction note: *Ibid.* **2006**, *110*, 12072.)
(82) Berard, J. J.; Schreckenbach, G.; Arnold, P. L.; Patel, D.; Love, J. B. *Inorg. Chem.* **2008**, *47*, 11583–11592.
(83) Schreckenbach, G.; Shamov, G. A. *Acc. Chem. Res.* **2010**, *43*, 19–29.
(84) Velde, G. T.; Bickelhaupt, F. M.; Baerends, E. J.; Guerra, C. F.; Van Gisbergen, S. J. A.; Snijders, J. G.; Ziegler, T. *J. Comput. Chem.* **2001**, *22*, 931–967.
(85) Guerra, C. F.; Snijders, J. G.; te Velde, G.; Baerends, E. J. *Theor. Chem. Acc.* **1998**, *99*, 391–403.
(86) Baerends, E. J.; Autschbach, J.; Bérces, A.; Bickelhaupt, F. M.; Bo, C.; Boerrigter, P. M.; Cavallo, L.; Chong, D. P.; Deng, L.; Dickson, R. M.; Ellis, D. E.; van Faassen, M.; Fan, L.; Fischer, T. H.; Fonseca Guerra, C.; van Gisbergen, S. J. A.; Götz, A. W.; Groeneveld, J. A.; Gritsenko, O. V.; Grüning, M.; Harris, F. E.; van den Hoek, P.; Jacob, C. R.; Jacobsen, H.; Jensen, L.; van Kessel, G.; Kootstra, F.; Krykunov, M. V.; van Lenthe, E.; McCormack, D. A.; Michalak, A.; Neugebauer, J.; Nicu, V. P.; Osinga, V. P.; Patchkovskii, S.; Philipsen, P. H. T.; Post, D.; Pye, C. C.; Ravenek, W.; Rodríguez, J. I.; Ros, P.; Schipper, P. R. T.; Schreckenbach, G.; Snijders, J. G.; Solà, M.; Swart, M.; Swerhone, D.; te Velde, G.; Vernooijs, P.; Versluis, L.; Visscher, L.; Visser, O.; Wang, F.; Wesolowski, T. A.; van Wezenbeek, E. M.; Wiesenekker, G.; Wolff, S. K.; Woo, T. K.; Yakovlev, A. L.; Ziegler, T. *ADF, ADF2008.01*; SCM, Theoretical Chemistry, Vrije Universiteit: Amsterdam, The Netherlands, 2008.
(87) Pye, C. C.; Ziegler, T. *Theor. Chem. Acc.* **1999**, *101*, 396–408.
(88) Klamt, A.; Jonas, V.; Burger, T.; Lohrenz, J. C. W. *J. Phys. Chem. A* **1998**, *102*, 5074–5085.
(89) van Lenthe, E.; Ehlers, A.; Baerends, E. J. *J. Chem. Phys.* **1999**, *110*, 8943–8953.
(90) van Lenthe, E.; Baerends, E. J.; Snijders, J. G. *J. Chem. Phys.* **1994**, *101*, 9783–9792.
(91) van Lenthe, E.; Baerends, E. J.; Snijders, J. G. *J. Chem. Phys.* **1993**, *99*, 4597–4610.

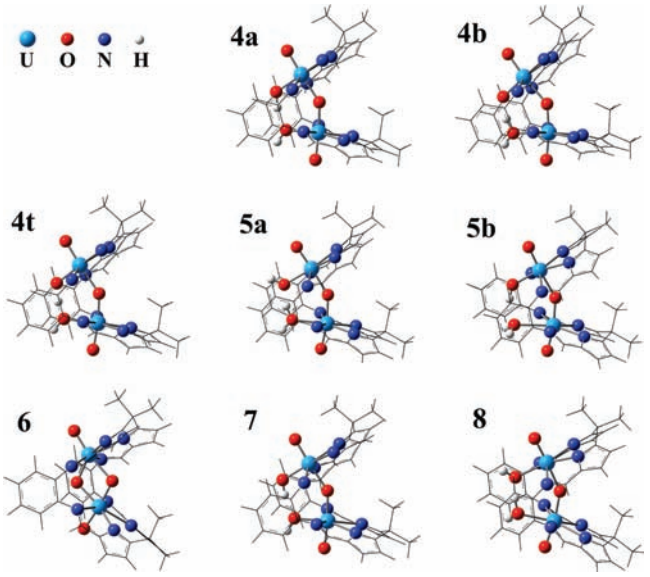

Figure 1. Optimized structures of binuclear hexa- and pentavalent uranium complexes.

unsaturated coordination sites of uranium(VI) along the equatorial plane. Below, we will further discuss the various reactions. The structures of optimized complexes, including three binuclear uranium(V) complexes, are depicted in Figure 1. Selected geometry parameters and bond orders are listed in Table 1. More detailed information about bond orders and atomic charges for **1**−**8** is given in the Supporting Information, Tables S2−S4. In the following, we shall discuss key geometrical features of the newly obtained uranium(VI) complexes. The uranium(V) complexes will be discussed in a separate section.

As shown in Scheme 2, the reactions of **2a** with water or hydronium result in a series of triangle-like O=U=O= U=O complexes, which resemble those of the experimentally reported binuclear V−O−V and Fe−O−Fe polypyrrolic complexes.[55,57] The hydroxyl and water groups bond to the uranium centers in the equatorial plane, with the exception of an equatorial oxo-group in **4b** (to be discussed later in more detail). All isomers of **4** and **5** display a six-membered ring geometry formed by the $U{=}O_{endo}{=}U$ unit and equatorial groups (Scheme 2 and Figure 1), which stabilize the complexes to some extent. **4a** is a slightly more energetically stable (0.69 kcal/mol) than **4b**. Three types of U−O bonds in **4a** were obtained as follows (Figure S1 of the Supporting Information and Table 1): (i) the $U{=}O_{exo}$ distances were calculated to be 1.82 and 1.81 Å and their bond orders were estimated to be 2.44 and 2.45; (ii) the predicted $U{-}O_{endo}$ bond lengths are 2.14 and 1.99 Å, corresponding to respective bond orders of 0.96 and 1.35; (iii) besides such axial U−O bonds, the equatorial U−O distances were estimated to be 2.04 and 2.18 Å with bond orders of 1.54 and 1.14, respectively. From the point of view of the calculated bond orders, the first group possesses a partial triple bond, and the other two groups are slightly stronger than a single bond. There is a hydrogen bond between the hydrogen of one hydroxyl group and the oxygen atom of another in **4a**. The 1.59 Å $H\cdots O_{eq2}$ distance falls within the range of typical hydrogen bonds.[92] Its bond order of 0.21 indicates that it is weaker than a normal single bond. The existence of this hydrogen bond inevitably weakens the $O_{eq1}{-}H$ interaction, resulting in a somewhat longer distance (1.03 Å) and smaller bond order (0.82) than those of $O_{eq2}{-}H$ (0.98 Å and 1.00) which are only slightly affected by the $H\cdots O_{eq2}$ hydrogen bonding.

The present calculations indicated that only a small amount of energy (1.28 kcal/mol) is required to form complex **4t** (Scheme 2). **4t** is a transition state with an imaginary frequency of 413i cm^{-1}. This mode was characterized as the $H\cdots O_{eq1}/O_{eq2}$ stretching vibration. In **4t**, the hydrogen atom is almost in the middle between the two equatorial oxygen atoms, as expected for the transition state of the proton transfer. As shown in Table 1 and Supporting Information, Figure S1, there are some accompanying changes in other geometry parameters and bond orders compared with those of **4a**.

Starting from **4a**, isomer **4b** can be formed by H^+ transfer via the transition state **4t**, Scheme 2. Compared with **4a**, one more U=O bond in **4b** was found with the characteristics of a partial triple bond: $U_1{=}O_{eq1}$ (1.91 Å distance with a bond order of 2.13), $U_1{=}O_{exo}$ (1.84 Å; bond order 2.44), and $U_2{=}O_{exo}$ (1.80 Å; bond order 2.44). On the other hand, the $U_1{-}O_{endo}$ and $U_2{-}O_{eq2}$ bond orders decrease to 0.60 and 0.61, respectively, comparable to a single bond, and there is an increase in the bond strength of $U_2{-}O_{endo}$ (1.74). From the bond orders shown in Supporting Information, Figure S1, **4b** features a structure with the cation−cation interaction of two uranyl units. Of most interest is an unusual combined *cis*- and *trans*-uranyl interaction, where the oxo atom of the *trans*-uranyl coordinates the uranium center of the *cis*-uranyl. The *trans*-uranyl is rendered five-coordinate in the equatorial plane by the bonding of an hydroxyl group bonds to the uranium atom of the *trans*-uranyl and the N_4-donor of the ligand. Similarly, the *cis*-uranyl displays overall 7-fold coordination: in addition to the two U=O bonds, there are four bonds from the polypyrrolic ligand and one from the *trans*-uranyl, although these five ligand bonds are of course not all in the equatorial plane.

As already discussed, the *trans*-uranyl structure is the most common structure in the experimentally reported uranyl complexes.[3−10] To the best of our knowledge, only one polymeric complex has been published with a supposed and controversial cis-uranyl structure, $[UO_2(Fadc)(THF)(Fc)]$ (fcdc = 1,2-ferrocenedicarboxylate, fc = ferrocene).[12,13] Additionally, bi- and polyuranyl cation−cation complexes were reported to have parallel structures (usually two *trans*-uranyl ions connected by oxygen bridges),[28,30,93−98] T-shaped structures (the uranium center of one *trans*-uranyl coordinated by the oxo

(92) Jeffrey, G. A. *An Introduction to Hydrogen Bonding* (*Topics in Physical Chemistry*); Oxford University Press: New York, 1997.

(93) John, G. H.; May, I.; Sarsfield, M. J.; Steele, H. M.; Collison, D.; Helliwell, M.; McKinney, J. D. *Dalton Trans.* **2004**, 734–740.

(94) Berthet, J. C.; Nierlich, M.; Ephritikhine, M. *Dalton Trans.* **2004**, 2814–2821.

(95) Alcock, N. W.; Flanders, D. J.; Pennington, M.; Brown, D. *Acta Crystallogr., Sect. C: Cryst. Struct. Commun.* **1988**, *44*, 247–250.

(96) Aberg, M. *Acta Chem. Scand.* **1969**, *23*, 791–810.

(97) Shvareva, T. Y.; Sullens, T. A.; Shehee, T. C.; Albrecht-Schmitt, T. E. *Inorg. Chem.* **2005**, *44*, 300–305.

(98) Charushnikova, I. A.; Den Auwer, C. *Russ. J. Coord. Chem.* **2007**, *33*, 53–60.

Table 1. Optimized Geometry Parameters and Bond Orders (in Parentheses) for Binuclear Hexa- and Pentavalent Uranium Complexes in the Gas Phase

	4a	4b	4t	5a	5b	6	7	8
				Bond Length (Å)				
U_1-O_{exo}	1.823 (2.44)	1.840 (2.44)	1.833 (2.44)	1.810 (2.46)	1.818 (2.45)	1.858 (2.42)	1.859 (2.39)	1.840 (2.42)
U_1-O_{endo}	2.144 (0.96)	2.341 (0.60)	2.256 (0.74)	2.130 (0.98)	2.226 (0.78)	2.107 (1.25) 2.144 (1.09)	2.158 (1.02)	2.158 (1.07)
U_1-N	2.535 (0.46) 2.455 (0.58)	2.544 (0.45) 2.474 (0.58)	2.538 (0.46) 2.466 (0.58)	2.508 (0.52) 2.409 (0.64)	2.513 (0.50) 2.419 (0.62)	2.616 (0.31) 2.586 (0.42)	2.661 (0.32) 2.569 (0.44)	2.622 (0.36) 2.497 (0.50)
U_1-O_{eq1}	2.041 (1.54)	1.911 (2.13)	1.961 (1.87)	2.186 (1.08)	2.066 (1.41)		2.104 (1.42)	2.253 (0.92)
$O_{eq1}-H$	1.025 (0.82)		1.205 (0.51)	0.977 (0.99)	0.989 (0.93)		1.006 (0.89)	0.973 (1.03)
U_2-O_{exo}	1.809 (2.45)	1.802 (2.44)	1.804 (2.44)	1.802 (2.47)	1.801 (2.45)	1.853 (2.43)	1.846 (2.44)	1.830 (2.45)
U_2-O_{endo}	1.994 (1.35)	1.898 (1.74)	1.932 (1.59)	1.998 (1.33)	1.939 (1.55)	2.151 (1.12) 2.078 (1.25)	2.030 (1.31)	2.038 (1.26)
U_2-N	2.539 (0.46) 2.463 (0.57)	2.541 (0.46) 2.442 (0.58)	2.542 (0.46) 2.453 (0.57)	2.513 (0.51) 2.409 (0.63)	2.481 (0.52) 2.394 (0.62)	2.629 (0.35) 2.582 (0.44)	2.657 (0.32) 2.585 (0.42)	2.611 (0.36) 2.497 (0.49)
U_2-O_{eq2}	2.177 (1.14)	2.382 (0.61)	2.284 (0.81)	2.381 (0.60)	2.687 (0.34)		2.027 (1.13)	2.431 (0.58)
$O_{eq2}-H$	0.976 (1.00)	1.056 (0.73) 0.974 (0.99)	1.211 (0.51) 0.975 (0.99)	1.048 (0.75) 0.975 (0.98)	0.985 (0.94) 0.985 (0.94)		0.973 (1.04)	1.075 (0.71) 0.975 (1.01)
$U_1\cdots U_2$	3.947 (0.17)	4.011 (0.13)	3.972 (0.15)	3.954 (0.17)	4.004 (0.15)	3.399 (0.49)	4.001 (0.19)	3.980 (0.20)
$H\cdots O$	1.589 (0.21)	1.450 (0.27)		1.485 (0.27)	1.865 (0.10)		1.691 (0.16)	1.405 (0.34)
$H\cdots O_{exo}(=U_1)$	2.474	2.402	2.444	2.546	2.459	2.905	2.382	2.540
				Bond Angle (deg)				
$O_{exo}-U_1-O_{endo}$	177.6	173.9	176.3	177.3	175.9	176.3/103.1	176.0	177.4
$O_{exo}-U_2-O_{endo}$	174.1	171.3	171.9	168.9	169.9	175.7/102.0	173.3	170.7
$U_1-O_{endo}-U_2$	145.1	142.1	142.9	146.5	147.9	107.2/105.9	145.7	146.1
$O_{endo}-U-O_{endo}$						73.2/73.6		

atom of another *trans*-uranyl),[24−26] as well as their combined arrangements.[27−29] However, there has not yet been a report about a combined *trans*- and *cis*-uranyl cation−cation complex in either experimental or theoretical studies.

Isomers **5a** and **5b** are formed when the hydronium attacks **2a**. As shown in Scheme 2, this can be completed in one step or two steps. In the latter case, one proton activates **2a** to form **2a-H**, and then a water molecule coordinates the uranium center and one $U-O_{endo}$ bond is broken concomitantly. Isomers **5a** and **5b** differ only in the arrangement of the equatorial water bonding to the U_2 atom. The former is about 10.70 kcal/mol more stable in total energy. They display the same coordination for the uranium atoms and thus have similar geometric parameters. Each of them exhibits, for instance, two shorter $U{=}O_{exo}$ distances of 1.81 Å (mean value), one long $U-O_{endo}$ bond length of 1.97 Å, and one even longer $U-O_{endo}$ distance of 2.20 Å. The hydroxyl group bonds strongly to one uranium atom, while the water coordinates another uranium atom weakly as shown in Table 1 and Supporting Information, Figure S1.

In all of these binuclear uranium(VI) complexes, the *trans*-dioxo uranyl unit stays almost linear (169°−178°), while the *cis*-dioxo uranyl angle is 98° in **4b**. The calculated $U_1-O_{endo}-U_2$ angles range from 142°−148°, and are correlated with the bite angle between the two N_4 planes of the Pacman ligand. The sum of these two angles roughly equals 180°. Therefore, our calculated $U_1-O_{endo}-U_2$ angles clearly pertain to the bite angles of 45°−62° in the synthesized binuclear U−M (M = Mn, Fe, and Co)[60] and M−M (M = Ti, V, Mn, Fe, Co, Ni, Cu, Zn, Pd, and Cd)[45−57] complexes.

All the calculated uranium complexes display two different kinds of equatorial N→U dative bonds, longer ones in the range of 2.48−2.54 Å and shorter ones ranging from 2.39 to 2.47 Å, similar to the experimental values of $(UO_2)(H_2L)(THF)$[59] and $[(THF)UO_2\cdots M(THF)](L)$ (M = Mn and Co).[60] Additionally, relatively short $U\cdots U$ separations of 3.95−4.01 Å were predicted for these binuclear complexes with calculated bond orders of 0.13−0.17. This may arise from the bridging oxygen atoms that pull the two uranium atoms proximate, and the bonding electron density localized on the U═O═U unit could contribute to the short $U\cdots U$ distance.

3.2. Energies of Formation Reactions of Binuclear Uranium(VI) Complexes. To study the thermodynamics of formation of the mono- and binuclear complexes indicated in Schemes 1 and 2, we chose $[UO_2(H_2O)_5]^{2+}$ to react with the polypyrrolic ligand. The corresponding reactions are listed in Table 2. We present the calculated total energies (ΔE), energies including zero point vibration energy (ΔE_0) and free energies (ΔG) of these reactions in Table 3. The $\Delta_r G$(gas/sol) for each complex is compared in Figure 2. We will begin with a discussion of the free energies in the gas phase.

Comparing the $\Delta_r G$(gas) value in Table 3 and Figure 2, the formation of **2a** from **1** is seen to be endothermic,[64] with the energy required computed as 38.56 kcal/mol. An additional 13.46 kcal/mol of energy is needed to form the isomer **2b**. Relative to the formation reaction of mononuclear **1** that is known experimentally, we can rationalize the destabilization of binuclear complexes from their structural features. The introduction of a second UO_2^{2+} ion into **1** to form **2a** results in a net consumption of energy. Several processes are energetically unfavorable, specifically breaking the bonds to the explicit first-shell (equatorial) waters around the uranyl ion, bending the linear *trans*-uranyl into the *cis*-uranyl, and eliminating the equatorial THF ligand. These energy losses are far higher than the energy that is released by the formation of $U{=}O_{endo}$ bonds. Although **2b** adopts a T-shaped arrangement with two *trans*-uranyls that avoids the energy cost of bending uranyl, more energy is required

Table 2. Formation Reactions of Mono- and Binuclear U(VI) Complexes on the Basis of the Polypyrrolic Ligand H_4L and Uranyl Complexes

reactions	products
$H_4L + [UO_2(H_2O)_5]^{2+} + THF \rightleftharpoons (UO_2)(THF)(H_2L) + 2H_3O^+ + 3H_2O$	**1**
$H_4L + 2[UO_2(H_2O)_5]^{2+} \rightleftharpoons (UO_2)_2(L) + 4H_3O^+ + 6H_2O$	**2a/2b**
$H_4L + 2[UO_2(H_2O)_5]^{2+} \rightleftharpoons [(U_2O_4H)(L)]^+ + 3H_3O^+ + 7H_2O$	**2a-H**
$H_4L + 2[UO_2(H_2O)_5]^{2+} \rightleftharpoons [(U_2O_3)(H_2O)(L)]^{2+} + 2H_3O^+ + 8H_2O$	**2a-2H/2b-2H**
$H_4L + 2[UO_2(H_2O)_5]^{2+} \rightleftharpoons [(U_2O_3)(L)]^{2+} + 2H_3O^+ + 9H_2O$	**3**
$H_4L + 2[UO_2(H_2O)_5]^{2+} \rightleftharpoons (UO_2)_2(H_2O)(L) + 4H_3O^+ + 5H_2O$	**4a/4b/4t**
$H_4L + 2[UO_2(H_2O)_5]^{2+} \rightleftharpoons (U_2O_3)(OH)(H_2O)(L)^+ + 3H_3O^+ + 6H_2O$	**5a/5b**

Table 3. Energies (kcal/mol) of the Formation Reactions of Mono- and Binuclear U(VI) Complexes in the Gas Phase, Together with the Calculated Free Energies of Solution Reactions ($\Delta_r G$(sol)) and the Free Energies of Solvation for Each Complex (ΔG(sol))

	1	**2a**	**2a-H**	**2a-2H**	**2b**	**2b-2H**	**3**	**4a**	**4b**	**4t**	**5a**	**5b**
$\Delta_r E$(gas)	46.64	143.08	79.31	89.95	155.52	108.02	123.66	137.35	138.04	138.62	66.18	76.87
$\Delta_r E_0$(gas)	40.53	126.44	61.31	70.79	139.07	88.59	101.90	121.90	122.48	121.39	49.70	60.74
$\Delta_r G$(gas)	24.29	62.85	−1.47	8.44	76.31	25.12	28.11	70.18	69.34	69.77	−2.32	8.23
$\Delta_r G$(sol)	21.28	49.37	53.29	36.51	63.69	86.51	85.23	63.73	62.01	63.49	5.80	62.89
ΔG(sol)[a]	−24.60	−27.27	−42.38	−152.42	−26.41	−119.10	−117.44	−26.17	−27.05	−26.00	−94.95	−48.41

[a] Solvation free energies for each complex.

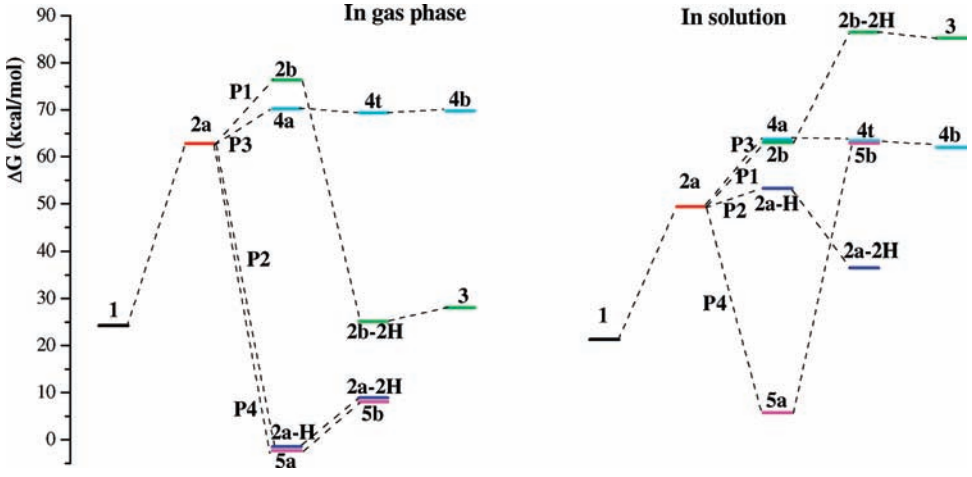

Figure 2. Free energies of formation reactions for binuclear U(VI) complexes on the basis of the polypyrrolic ligand and uranyl complexes in the gas phase and aqueous solution.

to force the Pacman ligand to increase the bite angle (open up further).[51] Starting from **2a**, the reactions in Paths 2 and 4 are thermodynamically favorable, involving proton-activating processes. Relative to **2a**, the formation of **2a-H** and **5a** give off energies of 64.32 and 65.17 kcal/mol, respectively. In contrast, energies of 6.49 kcal/mol or more must be provided to form isomers **4a**, **4b**, and **4t** (in Path 3), and double that energy (in Path 1) to form **2b**. As opposed to the exothermic proton-activating processes, the reactions in Path 3 need additional energy to break the original strong $U{=}O_{endo}$ bond in **2a** and form a weak equatorial HO−U bond in **4a** or H_2O−U bond in **4b**.

We shall now turn to the free energies of solvation for each complex, ΔG(sol) in Table 3. Because of the influence of the solvent environment on chemical reactions, the thermodynamic calculations in the gas phase inevitably deviate from those involved in the real experimental reactions. Herein, we employed the COSMO solvent model in the ADF code to account for the behavior of uranium complexes in aqueous solution. Calculations indicate that solvation stabilizes the uranium complexes to different degrees. The solvation free energy ΔG(sol) depends on the charge distribution of the complexes that can be represented by the charges, dipole moments, and higher multipole moments. As far as the charge is concerned, solvation free energies were calculated at about −25 kcal/mol for the neutral complexes (**1**, **2a**, **2b**, **4a**, **4b**, and **4t**), whereas those of the positively charged complexes were estimated at about −50 and −120 kcal/mol for the +1 and +2 systems, respectively (Table 3). It is worth noting that **5a** (with +1 charge) and **2**−**2H** (+2 charge) have even higher solvent stabilization than the other complexes with the same charge. They correspond to solvation energies of −94.95 and −152.42 kcal/mol, respectively. We attribute the solvation stabilization to

the charge distribution that is correlated with structural features of the complex. Different structures for complexes with the same overall charge allow the charge to be more or less evenly distributed, resulting in dipole moments of differing magnitude. Among the complexes with a +1 charge, **2a-H** features a four-membered ring structure of U=O=U=O, while **5a** and **5b** display a six-membered ring skeleton as shown in Scheme S1 of Supporting Information. Thus it is easier to disperse the positive charge in **5** than in **2a-H**. The high symmetry in **5a** results in more pronounced charge dispersion than in its isomer **5b**. The charge of the hydrogen atoms bonding to the rings (in Supporting Information, Scheme S1) could intuitively illustrate the positive charge distribution in the complex. Among the complexes with a +2 charge, **2a-2H**, **2b-2H**, and **3**, the first one has the highest solvation stabilization. This can be rationalized as follows. On one hand, a stabilization of **2a-2H** results from the U=O=U$\cdots$ OH_2 ring structure. On the other hand, **2a-2H** has a special structure where the water tends to depart from the bulky part of uranium complex. The calculated H_2O-U distance of 2.70 Å is significantly longer than other known equatorial U−O distances (ca. 2.55 Å).[6,9,13,24,26,93−97] This feature increases the polarity of **2a-2H** and results in a particularly strong interaction with the polar aqueous solvent.

The different solvation free energies of the individual complexes will lead to changes in the free energies of the reactions. In other words, the inclusion of solvation changes the free energy of the formation reaction for each complex (in Table 3 and Figure 2). Comparing the reaction free energies between the gas phase, $\Delta_r G$(gas), and solution, $\Delta_r G$(sol), there are indeed some marked differences. First, solvation stabilizes the formation reactions of neutral complexes. Among them, **2a** has the largest decrease of its reaction energy at 13.48 kcal/mol, whereas the energy for **1** is only lowered by 3.01 kcal/mol. The net effect is that the formation of **2a** from **1** becomes easier in the solution than in the gas phase, although it is still calculated to be endothermic. Second, solvation destabilizes the formation reactions of charged systems, thus more energy is required to form them in solution. The increase of the reaction energies $\Delta_r G$(sol) amounts to over 54 kcal/mol for the charged complexes, except for **5a** and **2a-2H** which have increases of 8.12 and 28.07 kcal/mol, respectively. Relative to **2a** in solution (Figure 2), only the formation reactions of **2a-2H** and **5a** are thermodynamically favorable, giving off 12.86 and 43.57 kcal/mol energies, respectively. In summary, solvation in a polar solvent increases the possibility of the reaction **1**→**2a** relative to the gas phase by making it less endothermic, and makes the subsequent reactions of **2a** more difficult, although **2a**→**5a** and **2a**→**2a-2H** are still exothermic.

A comparison among the ΔG(sol) of reagents and products, especially the charged species in the formation reactions, can be used to qualitatively interpret the difference between $\Delta_r G$(sol) and $\Delta_r G$(gas). In the formation reactions of neutral complexes (**1**, **2**, and **4**, Table 2), $[UO_2(H_2O)_5]^{2+}$ and H_3O^+ are the charged systems, with corresponding ΔG(sol) values of −89.28 and −190.71 kcal/mol, respectively. There is only about 5 kcal/mol difference per unit positive charge. This can be understood from the opposite effects of charge and size in $[UO_2(H_2O)_5]^{2+}$ and $2H_3O^+$. To first order, the solvation stabilization is proportional to the square of the charge and inversely proportional to the distance between charge and polarizable medium. (This model would be exact for a point charge within the center of a spherical cavity.) $[UO_2(H_2O)_5]^{2+}$ has a charge of 2+, resulting in a factor of 4 in solvation free energy relative to the 1+ charge of H_3O^+. However, the solute radius of the latter is roughly 1/2 that of the former. Overall, the effects of charge and size cancel out approximately between $[UO_2(H_2O)_5]^{2+}$ and H_3O^+. Thus, the solvation free energy ΔG(sol) of the neutral complexes **1**, **2**, and **4** at about −25 kcal/mol plays an important role in their formation reactions, making $\Delta_r G$(sol) lower than $\Delta_r G$(gas).

In contrast, three charged species, $[UO_2(H_2O)_5]^{2+}$, H_3O^+, and the respective charged binuclear complex, are present in the formation reactions of the charged complexes (Table 2). As discussed above, half of ΔG(sol) of $[UO_2(H_2O)_5]^{2+}$ is close to that of H_3O^+. If the remaining small difference is neglected, the destabilization of $\Delta_r G$(sol) relative to $\Delta_r G$(gas) will be approximately proportional to

$$\Delta G(\text{sol})\{\text{complex}\} - 1/2\Delta G(\text{sol})\{[UO_2(H_2O)_5]^{2+}\}$$

and

$$\Delta G(\text{sol})\{\text{complex}\} - \Delta G(\text{sol})\{[UO_2(H_2O)_5]^{2+}\}$$

for the formation reactions of the +1 and +2 charged complexes, respectively. As mentioned, the solvation free energy is proportional to the square of the charge and inversely proportional to the distance between charge and polarizable medium. Therefore, the destabilization of $\Delta_r G$(sol) relative to $\Delta_r G$(gas) can be qualitatively characterized as

$$(1/r_c - 2/r_u) = (1/r_c - 1/r_u) - 1/r_u$$

for +1 charged complex and

$$4 * (1/r_c - 1/r_u)$$

for +2 charged complex, where r_c and r_u denote the distances between charge of the complex or aqua uranyl ion and the polarizable medium. Because of its much shorter r_u distance,[77] $[UO_2(H_2O)_5]^{2+}$ is significantly more strongly stabilized by solvation than the charged complex. Therefore, the formation reactions of charged systems are destabilized by solvation with respect to those in the gas phase.

3.3. Binuclear Uranium(V) Complexes. In the calculations of the above binuclear uranium(VI) complexes, three pairs of isomers, **2a**/**2b**, **4a**/**4b**, and **5a**/**5b**, were obtained, all of which correspond to stationary points on the potential energy surface. From these starting structures, we also attempted to optimize their uranium(V) analogues. However, only the more stable isomer in each pair was found to correspond to a stable uranium(V) complex. These are labeled as **6**, **7**, and **8**, respectively. In the calculations on these binuclear uranium(V) complexes, the two single electrons can adopt either spin

parallel or spin antiparallel states. Isomer **6** was optimized with both spin states, and it was found that the calculated geometry parameters, bond orders, and atomic charges are very close (Supporting Information, Table S5), the only difference being the spin density around the two uranium atoms. Therefore, only the optimized geometries of **6**−**8** with the state of two spin-parallel electrons will be discussed.

Atomic charges and electron-spin densities for these complexes are listed in the Supporting Information, Table S4. Comparing the calculated uranium charges of the U(VI) complexes with their U(V) analogues, we find that the charges of U(VI) are more positive, 0.14−0.29 higher than those of the U(V) counterparts. Nevertheless, all of these charges are far lower than the formal oxidation states of uranium (+6 and +5, respectively). In contrast, the calculated electron-spin density provides a more direct evidence for the oxidation state of uranium atom. The uranium(V) complexes have electron-spin densities of about 1.10−1.14 localized around the uranium atoms (Supporting Information, Table S4), corresponding to one single uranium 5f electron, but have electron spin densities of approximately zero for other atoms (for instance, ca. 0.01−0.06 for the oxygen atoms). We find zero electron-spin densities for the uranium atom of the uranium(VI) complexes, in accordance with the $U(4f^{14}5d^{10}6s^{2}6p^{6})$ closed-shell system.

We present the calculated geometry parameters and bond orders of binuclear uranium(V) complexes **6**, **7**, and **8** in Table 1 and Figure 1. Geometrical features similar to the U(VI) species (**2a**, **4a**, and **5a**) were found, that is, two shorter $U{=}O_{exo}$ distances with the characteristics of a partial triple bond and two longer $U{=}O_{endo}$ bond lengths (four for **6**) with bond orders above 1.00. Upon reduction from U(VI) to U(V), most distances lengthen with the exception of two $U{=}O_{endo}$ bonds in complex **6**. For example, the $U{=}O_{exo}$ bond lengths increase by about 0.03−0.05 Å while the U−N bonds lengthen even more, by about 0.09−0.14 Å. This agrees with the trend found in the previous calculations on $[U^{VI}O_2(H_2O)_5]^{2+}$ and $[U^{V}O_2(H_2O)_5]^{+}$.[81] In addition, we find that the calculated $U_1{=}O_{exo}$ distance is longer than the $U_2{=}O_{exo}$ one in each complex because the oxygen atom of the former is involved in hydrogen bonding (Table 1).

4. Conclusions

We carried out relativistic density functional theory calculations on a series of binuclear hexa- and pentavalent uranium complexes. Explicit and implicit solvent effects were taken into account. Four reaction pathways were designed to investigate the formation of binuclear uranium(VI) complexes from the starting complex **2a**. The most important points are as follows:

The present calculations indicate that the butterfly like **2a** is highly reactive. Its structure resembles the newly synthesized polypyrrolic complex, $[(UO_2)(OH)K(THF)_2(H_2L^{Me})]$.[65] Several new complexes were predicted to result from the reactions induced by water (Path 3) and hydronium (Path 4). A pair of isomers, **4a** and **4b**, can be converted via a transition state **4t**, with an energy barrier of less than 1.5 kcal/mol; **4b** has an unusual combined *cis*-uranyl/*trans*-uranyl cation−cation structure, where the oxo atom of the *trans*-uranyl coordinates the uranium center of the *cis*-uranyl. However, the more stable isomer, **4a**, features two hydroxyl groups linked to two separate uranium atoms. Another pair of isomers, **5a** and **5b**, differ in their arrangements of the equatorial water that bonds to the U_2 atom; **5a** is about 10.70 kcal/mol more stable in total energy.

In conjunction with previous studies,[64] the free energies of reactions of **2a** induced by isomerization (Path 1), a proton (Path 2), water (Path 3), and hydronium (Path 4) were calculated in the gas phase and aqueous solution. In the gas phase, Paths 2 and 4 are feasible as far as $\Delta_r G$(gas) of the complexes are concerned. The inclusion of solvent effects stabilizes all the complexes and leads to easier formation of binuclear **2a** from mononuclear **1** and uranyl species. However, only the reaction processes of **2a**→**5a** in Path 4 and **2a-H**→**2a-2H** in Path 2 are thermodynamically favorable in solution. In the formation reactions of the neutral complexes, the free energies of solvation ΔG(sol) of the complexes play an important role, making $\Delta_r G$(sol) lower than $\Delta_r G$(gas). However, the stronger solvation stabilization of $[UO_2(H_2O)_5]^{2+}$ relative to that of the charged complexes results in the destabilization of $\Delta_r G$(sol) relative to $\Delta_r G$(gas), in agreement with a simple, qualitative solvent-effect model. In general terms, these studies elucidate the reactivity and stability of uranyl complexes theoretically, and provide guidance for further tuning the types of complexes.

In the above reactions, three pairs of isomers were obtained for binuclear uranium(VI) complexes, but only the most stable one in each pair was found for binuclear uranium(V) analogues. It is evident that the polypyrrolic ligand can stabilize U(V) species, supporting the experimentally reported U(V) analogues.[61,62] The electron-spin density localized on the uranium(V) atom was calculated to be in the range of 1.10−1.14, which provides direct evidence for the +5 oxidation state of the uranium atom. The U(V) complexes exhibit geometrical features similar to their respective U(VI) counterparts; most bonds lengthen upon reduction from U(VI) to U(V), in agreement with previous calculations on $[U^{VI}O_2(H_2O)_5]^{2+}$ and $[U^{V}O_2(H_2O)_5]^{+}$.[81] In subsequent studies, we plan to focus on binuclear homo- or heterovalent uranium complexes with oxidation states III−VI and their redox potentials.

Acknowledgment. G.S. would like to thank Polly Arnold and Jason Love for inspiration, encouragement, and helpful discussions. The authors acknowledge Scott Kroeker for help with the manuscript and Dimitri Laikov for providing us with the Priroda code. This research has been enabled by the use of computing resources provided by WestGrid and Compute/Calcul Canada. Financial support from the Natural Sciences and Engineering Research Council of Canada (NSERC) is gratefully acknowledged.

Supporting Information Available: Tables of geometry parameters, bond orders, and atomic charges for mono- and binuclear complexes (**1**, **2a**, **2b**, **2a-H**, **2a-2H**, **2b-H**, and **3**); table of geometry parameters of **1** and **2a** optimized by Priroda (in gas phase) and ADF (in gas phase and solution) code; table of atomic charges for **4**−**8** together with electron-spin densities for binuclear U(V) complexes. Table of geometry parameters of **6** with electron spin parallel and spin antiparallel states. Scheme for structural features of positively charged complexes and the atomic charges of hydrogen atoms. Figure of the U−O and H−O bond orders of binuclear uranium(VI) complexes. This material is available free of charge via the Internet at http://pubs.acs.org.